Journal of Materials Chemistry B

Hydrosulfide-methaemoglobin-albumin cluster: A hydrogen sulfide donor

Journal:	*Journal of Materials Chemistry B*
Manuscript ID	TB-ART-07-2024-001621.R1
Article Type:	Paper
Date Submitted by the Author:	02-Oct-2024
Complete List of Authors:	Suzuki, Yuto; Keio Gijuku Daigaku Yamada, Taiga; Chuo University Faculty of Science and Engineering Graduate School of Science and Engineering Enoki, Yuki; Keio University Matsumoto, Kazuaki; Keio University Faculty of Pharmacy Graduate School of Pharmacy Komatsu, Teruyuki; Chuo University Faculty of Science and Engineering Graduate School of Science and Engineering, Department of Applied Chemistry Taguchi, Kazuaki; Keio University Faculty of Pharmacy Graduate School of Pharmacy,

ARTICLE

Hydrosulphide-methaemoglobin-albumin cluster: A hydrogen sulphide donor

Received 00th January 20xx,
Accepted 00th January 20xx

DOI: 10.1039/x0xx00000x

Yuto Suzuki[a], Taiga Yamada[b], Yuki Enoki[a], Kazuaki Matsumoto[a], Teruyuki Komatsu[b], Kazuaki Taguchi*[a]

Methaemoglobin (metHb) possesses inherent characteristics that facilitate reversible binding to hydrogen sulfide. Exogenous hydrogen sulfide supplementation imparts beneficial bioactive effects, including antioxidant and anti-inflammatory; hence, we hypothesized that the metHb-hydrogen sulfide complex could act as a hydrogen sulfide donor for medication. In this study, we prepared a hydrosulfide-metHb-albumin (H_2S-metHb-albumin) cluster and examined its applicability as a hydrogen sulfide donor in the mice model of hepatic ischemia-reperfusion injury. Structural analysis revealed that the H_2S-metHb-albumin cluster exhibited a nanostructure wherein one metHb was wrapped by an average of three albumins, and hydrogen sulfide was bound to the haem. Additionally, the H_2S-metHb-albumin cluster exhibited low-pH responsiveness, leading to sustained release of hydrogen sulfide. Owing to these structural and pharmaceutical characteristics, the severity of hepatic ischemia-reperfusion injury was alleviated via antioxidant and anti-inflammatory effects of the H_2S-metHb-albumin cluster treatment. The protective effects were more potent in the H_2S-metHb-albumin cluster compared to that in a conventional hydrogen sulfide donor (sodium hydrogen sulfide). No abnormal signs of toxic and biological responses were observed after the H_2S-metHb-albumin cluster administration, confirming high biological compatibility. These results successfully establish the proof of concept that the H_2S-metHb-albumin cluster is a promising hydrogen sulfide donor. To the best of our knowledge, this is the first report demonstrating the remarkable potential of metHb as a biomaterial for hydrogen sulfide donors.

1. Introduction

Exposure to hydrogen sulphide, a gaseous molecule, in massive quantities, induces acute poisoning *via* inhibition of cytochrome *c* oxidase. However, low levels of hydrogen sulphide are constantly produced in the body for maintaining homeostasis because it functions as a signalling molecule and cytoprotective factor [1,2]. Several studies have demonstrated that these beneficial bioactive effects can be achieved via exogenous hydrogen sulphide supplementation in various animal models of disease and disorder [3–7]; therefore, hydrogen sulphide is expected to be crucial for drug development. Sodium hydrogen sulphide (NaHS) is used as a hydrogen sulphide donor for basic and applied investigations of hydrogen sulphide [8–11]. However, using conventional donors to provide hydrogen sulphide for the disorder therapy is unfavourable owing to their drawbacks, such as tissue nonselectivity, non-sustained effects, and the risk of hydrogen sulphide poisoning [12–14]. Thus, frequent administration and monitoring of systemic conditions are required for using conventional hydrogen sulphide donors *in vivo*. Moreover, the total dosage quantity is restricted to avoid hydrogen sulphide poisoning, which is a substantial challenge to achieving sufficient therapeutic effects. To overcome these limitations, hydrogen sulphide donors from low-molecular weight to macromolecule have been developed for producing hydrogen sulphide-based medications [15].

Methaemoglobin (metHb) is an oxidized form of haemoglobin (Hb) containing ferric iron (Fe^{3+}) at the centre of haem. Binding studies of metHb have revealed that hydrogen sulphide reversibly binds to metHb with high affinity, but the binding strength decreases in a low-pH environment [16,17]. Hence, we hypothesized that metHb could act as a potential scaffold for hydrogen sulphide in response to low pH. However, two challenges must be overcome for using metHb as a hydrogen sulphide delivery system: first involves clearance from glomerular filtration, which causes renal oxidative damage due to reactive oxygen species (ROS) *via* accumulated haem [18] and the other is its extremely short half-life (approximately 2 h)[19] because metHb is rapidly cleared from circulation *via* the haptoglobin-CD163 axis in the liver and renal glomerular filtration [20]. Therefore, pharmaceutical ingenuity is essential for establishing the metHb-based hydrogen sulphide delivery system. We previously developed metHb-albumin clusters, wherein metHb was surrounded by human serum albumin (HSA) acting as a detoxifying agent for hydrogen sulphide [21]. HSA modification of the metHb surface prolonged its blood retention without renal damage. Additionally, metHb-albumin clusters maintained a comparable binding characteristic with hydrogen sulphide to metHb, facilitating the utilization of metHb-albumin clusters as scaffolds for metHb-based hydrogen sulphide donors.

[a] *Division of Pharmacodynamics, Keio University Faculty of Pharmacy, 1-5-30 Shibakoen, Minato-ku, Tokyo 105-8512, Japan.*
[b] *Department of Applied Chemistry, Faculty of Science and Engineering, Chuo University, 1-13-27 Kasuga, Bunkyo-ku, Tokyo 112-8551, Japan.*
† Footnotes relating to the title and/or authors should appear here.
Supplementary Information available: [details of any supplementary information available should be included here]. See DOI: 10.1039/x0xx00000x

Further, this novel donor offers several advantages over other hydrogen sulphide donors, including effective hydrogen sulphide release at a low-pH site, no environmental pollution owing to the inherent characteristics of metHb, and using green materials (proteins derived from living organisms).

In this study, we attempted to establish a proof-of-concept that the hydrosulphide-metHb-albumin (H_2S-metHb-albumin) cluster acts as a hydrogen sulphide donor. To this end, we first prepared an H_2S-metHb-albumin cluster and evaluated its structural and pharmaceutical characteristics, including hydrogen sulphide release. Next, the applicability of hydrogen sulphide donors was assessed in a mouse model of hepatic ischemia-reperfusion injury (IRI). Finally, the biological compatibility and toxicity of the H_2S-metHb-albumin clusters were examined in healthy mice. The experimental results also demonstrate a proof-of-concept for using metHb as a potential biomaterial for hydrogen sulphide donors.

2. Experimental

2.1. Preparation of H_2S-metHb-albumin cluster

Hb-albumin clusters (5 g Hb/dL in phosphate-buffered saline (PBS), pH 7.4) were synthesized by conjugating bovine Hb (Tokyo Shibaura Zouki Co., Ltd., Tokyo, Japan) and HSA (Japan Blood Products Organization, Japan) *via* *N*-succinimidyl 3-maleimido-propionate (FUJIFILM Wako Pure Chemical, Osaka, Japan), as depicted in Fig. 1a [22]. Hb-albumin clusters and sodium nitrite ($NaNO_2$; Nacalai Tesque, Inc., Kyoto, Japan) were mixed, followed by incubation to yield a metHb-albumin cluster solution, as reported previously (Fig. 1b)[21]. H_2S-metHb-albumin cluster solution was prepared by adding an excess quantity of NaHS (Sigma-Aldrich, St. Louis, USA) to the metHb-albumin cluster (Fig. 1c). The addition of H_2S to metHb was confirmed by a change in the Ultraviolet-visible (UV-vis) spectra recorded on the UV-vis spectrometer (UV-1900i, Shimadzu, Japan). Unreacted NaHS was removed using a centrifuge (Amicon Ultra-15; 50 *kDa* MWCO, Merck Millipore, USA). H_2S-metHb-albumin cluster was prepared before usage in all experiments without storage.

2.2. Determination of structural characteristics

The structures of the H_2S-metHb-albumin clusters were characterized by a comprehensive analysis using UV-vis. spectroscopy, dynamic light scattering, size-exclusion chromatography (SEC), circular dichroism (CD), and Native-PAGE. The detailed methods and instruments used are provided in Supporting Information.

2.3. In vitro sulphide release

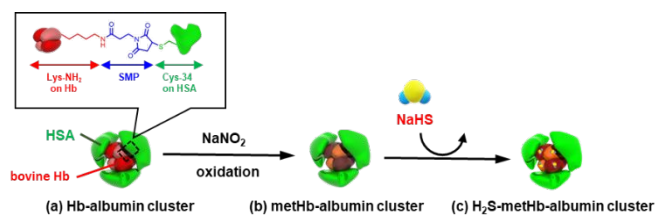

Figure 1 Schematic illustration of the H_2S–metHb-albumin cluster preparation.

H_2S-metHb-albumin cluster (500 mg metHb/dL) in 100 mM phosphate buffer (pH 7.4, 6.8, and 6.2) or fetal bovine serum (Thermo Fisher Scientific, Waltham, MA, USA) were incubated at 37 °C. Every hour for 12 h, the samples were diluted to 2 µM, and subsequently, metHb and H_2S-metHb-derived absorbance (423.5 nm) were measured using a UV-vis. spectrometer. The sulphide release ratio was calculated using the following equation (1):

$$\text{Sulphide release (\%)} = \{1 - (ABS_t - ABS_{baseline}) / (ABS_0 - ABS_{baseline})\} \times 100 \quad (1)$$

where ABS_t and ABS_0 are the absorbances at 423.5 nm measured at a specific time point and before incubation (0 min), respectively. The absorbance value of the metHb-albumin cluster at 423.5 nm, which is the final form after 100% H_2S release from H_2S-metHb-albumin clusters, is known as the $ABS_{baseline}$.

2.4. Animal ethics

All animal experimental protocols were approved by the Institutional Animal Care and Use Committee of the Keio University (A2022–347). Male ICR mice (7 weeks old; Japan SLC, Inc., Shizuoka, Japan) were used for all the animal experiments in the present study.

2.5. Maximal tolerance dose of H_2S-metHb-albumin cluster

Either the H_2S-metHb-albumin cluster (100 (0.35), 200 (0.69), 300 (1.05), 400 (1.39), 500 (1.74), and 600 (2.09) mg metHb/kg (mg NaHS/kg)) or NaHS (0.35, 0.69, 1.05, 1.39, 1.74, and 2.09 mg NaHS/kg) were administered to healthy mice (n=5 per group), and their survival at 24 h was observed.

2.6. Efficacy of H_2S-metHb-albumin cluster against hepatic IRI

The mice received H_2S-metHb-albumin clusters (100 (0.35), 300 (1.05), and 600 (2.09) mg metHb/kg (mg NaHS/kg)), NaHS (1.05 mg NaHS/kg), metHb-albumin clusters (300 mg metHb/kg), or saline under 2.5% isoflurane anaesthesia. After 30 min, the IRI procedure was performed on all the mice, according to a previously published report [23]. Briefly, the mice underwent midline laparotomy, and the hepatic triplet (portal vein, hepatic artery, and bile duct) was clamped with an atraumatic clip to achieve 70% hepatic ischemia under 2.5% isoflurane anaesthesia. The mice were kept anesthetized (2.5% isoflurane) during ischemia, and their body temperature was controlled using a heater mat. The microvascular clamp was removed 45 min after ischemia began, and the mice were awakened from anaesthesia. The sham mice were subjected to the same procedure without clamping. At 6 h reperfusion, the mice were sacrificed, and samples (blood and liver) were collected for evaluation. The collected blood samples were used to determine the levels of aspartate aminotransferase (AST), alanine aminotransferase (ALT), and cytokines in plasma. The harvested livers were used to evaluate the morphology, glutathione (GSH), GSH-to-oxidized GSH (GSSG) ratio (GSH/GSSG), and malondialdehyde (MDA) concentration. Detailed methods, instrumentation, and reagents used have been described in the Supporting Information.

2.7. Assessment of biological compatibility and toxicity

The H_2S-metHb-albumin clusters (300 (1.05) mg metHb/kg (mg NaHS/kg)) were intravenously injected into healthy mice under 2.5% isoflurane anaesthesia. Biological samples (blood, liver, and kidneys) were collected 1, 3, 7, and 14 days after injection. Analysis of biochemical parameters were conducted by the Oriental Yeast Industry Co. (Tokyo, Japan). The morphologies of the liver and kidneys were observed after haematoxylin and eosin (H&E) staining using a BZ-X700 microscope (Keyence Corp., Japan). Biological samples collected from four healthy mice 14 days after saline administration were used as controls.

Further, biological samples (blood, heart, lungs, liver, kidneys, and brain) were collected from mice administered with H_2S-metHb-albumin clusters (300 (1.05) mg metHb/kg (mg NaHS/kg)) at 10, 30, 60, and 180 min after injection. Blood gas parameters were analysed using RAPID Point® 500 (Siemens Healthcare Diagnostics, Germany). Cytochrome *c* oxidase activities were measured using the method described previously [24,25].

2.8. Data analyses

Student's *t*-test, Dunnett's test, or one-way analysis of variance (ANOVA), followed by the Tukey-Kramer multiple comparison test, were used to analyse statistical significance. Data with a *p* value <0.05 were considered significant.

3. Results and Discussion

3.1. Structural and physicochemical characteristics of H_2S-metHb-albumin cluster

The structure of the metHb-albumin cluster exhibited that one metHb was covalently wrapped by an average of three HSA molecules [21]. Understanding the cluster structure and physicochemical properties is crucial for acquiring advantages over metHb (long blood retention and no renal damage); therefore, we evaluated the structural and physicochemical properties of the H_2S-metHb-abumin cluster. The absorbance peak of the UV-vis spectrum shifts from 405 to 423.5 nm upon the addition of hydrogen sulphide to the metHb-albumin cluster (Fig. 2a). The absorption at 405 and 423.5 nm could be attributed to the ferric haem and H_2S-(ferric haem) complex, respectively [17], indicating that metHb-albumin cluster loads hydrogen sulphide by one-pot addition of NaHS. However, the physicochemical properties (Table 1) and particle size distribution (Fig. 2b) of the H_2S-metHb-albumin cluster are similar to those of the metHb-albumin cluster, indicating no aggregation or degradation occurs after hydrogen sulphide loading. Additionally, the SEC chromatograms (Fig. 2c), band patterns in Native-PAGE (Fig. 2d), and CD spectral shapes (Fig. 2e) are similar for metHb-albumin and H_2S-metHb-albumin clusters. Several peaks and bands are observed in the SEC chromatograph and Native-PAGE owing to several clusters in the metHb-albumin cluster solution, wherein one metHb is wrapped with one to four HSA molecules[21]. The CD spectrum of the H_2S-metHb-albumin cluster agrees well with that obtained by the integration of one metHb and three HSA molecules, indicating that the average number of HSA molecules conjugated with metHb in the H_2S-metHb-albumin cluster is three, similar to that of the metHb-albumin cluster [22]. Hence, the overall structure of the H_2S-metHb-albumin cluster is similar to that of the metHb-albumin cluster.

The metHb possesses inherent reversible binding properties to hydrogen sulfide[16]. Additionally, the binding affinity of hydrogen sulphide declines as the pH decreases [17]. Therefore, the H_2S-metHb-albumin cluster can rapidly release sulphide at low pH. As expected,

Table 1 Physicochemical parameters.

	Diameter (nm)	PDI	ζ-potential (mV)
H_2S-metHb-albumin cluster	13.9 ± 0.05	0.04 ± 0.01	-3.11 ± 0.11
metHb-albumin cluster	14.1 ± 0.10	0.04 ± 0.01	-3.07 ± 0.09
HSA	6.8 ± 0.04	0.02 ± 0.01	-3.20 ± 0.33
metHb	5.9 ± 0.04	0.12 ± 0.01	-4.98 ± 0.44
H_2S-metHb	6.0 ± 0.16	0.12 ± 0.03	-4.91 ± 0.37

HSA: human serum albumin, metHb: methaemoglobin, PDI: polydispersity index.
n = 3, mean ± S.D.

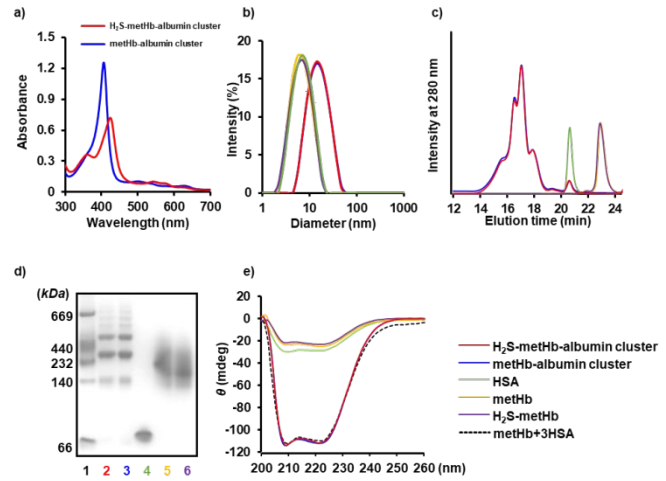

Figure 2 Representative results for structural analysis of H_2S–metHb-albumin cluster. a) UV-vis spectra, b) particle size distribution, c) SEC chromatograms, d) Native–PAGE, and e) CD spectra. The numbers of Native-PAGE reveal loaded-sample as follows: 1: marker, 2: H_2S–metHb-albumin cluster, 3: metHb-albumin cluster, 4: human serum albumin (HSA), 5: methaemoglobin (metHb), and 6: H_2S–metHb. Experiments were repeated, exhibiting similar results at least three times.

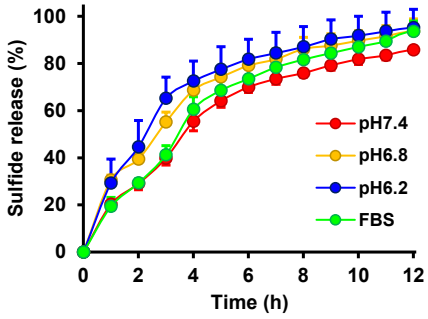

Figure 3 Time course of sulphide release from H_2S–metHb-albumin cluster in FBS and PBS at different pH conditions. n = 3, mean ± S.D.

Table 2 Survival after intravenous single administration of NaHS (groups A–F) and H_2S-metHb-albumin cluster (groups G–L) at different doses.

Group	Dose		Survival (%)
	metHb (mg/kg)	NaHS (mg/kg)	
A	–	0.35	100
B	–	0.69	100
C	–	1.05	100
D	–	1.39	100
E	–	1.74	80
F	–	2.09	0
G	100	0.35	100
H	200	0.69	100
I	300	1.05	100
J	400	1.39	100
K	500	1.74	100
L	600	2.09	100

n= 5 per group

H_2S-metHb-albumin cluster releases sulphide over time, releasing 50% in 3.69 ± 0.24 and 3.36 ± 0.17 h in physiological pH buffer (PBS, pH 7.4) and fetal bovine serum (FBS), respectively (Fig. 3). Further, the sulphide release rate of H_2S-metHb-albumin cluster is facilitated by a decrease in pH (50% sulphide release: 2.18 ± 0.46 and 2.73 ± 0.22 h at pH 6.2 and 6.8, respectively). Hence, the H_2S-metHb-albumin cluster emerges as a promising hydrogen sulphide donor, especially for treating diseases with focal sites at low pH.

3.2. Maximal tolerated dose of H_2S-metHb-albumin cluster

The effect of exogenous hydrogen sulphide exposure on the body exhibits Yin-Yang modalities in a concentration-dependent manner: low-dose exposure exhibits beneficial bioactive effects, whereas rapid high-dose exposure leads to lethal acute poisoning[26]. Therefore, determining the maximal tolerated dose of hydrogen sulphide donors is essential to ensure safety prior to their application in disorder therapy. All mice administered with the conventional hydrogen sulphide donor, NaHS, survive up to a dosage of 1.39 mg/kg (Table 2A-D). However, one mouse and all mice die at NaHS doses of 1.74 and 2.09 mg/kg, respectively (Table 2E and F). In contrast, no deaths are observed for up to 600 mg metHb/kg of the H_2S-metHb-albumin cluster, which contains 2.09 mg/kg of NaHS (Table 2G–L). Therefore, the H_2S-metHb-albumin cluster inhibits the induction of hydrogen sulphide poisoning even when a high dose of hydrogen sulphide is administered, at which NaHS induces lethal hydrogen sulphide poisoning. The H_2S-metHb-albumin cluster releases sulphide in a sustained-release manner (Fig. 3), which prevents a rapid increase in the hydrogen sulphide concentration in the body. Hence, the H_2S-metHb-albumin cluster can be used more safely than the NaHS when high doses of hydrogen sulphide are required for disease therapy. Additionally, the dose volume of H_2S-metHb-albumin clusters is expected to exceed 600 mg metHb/kg (12 mL/kg), which unfortunately increases the cardiovascular burden. The dose volume of the solution can be decreased by increasing the product concentration of the metHb-albumin cluster to more than 5 g metHb/dL; however, it is not recommended due to its high viscosity. Therefore, the maximal tolerated dose of the H_2S-metHb-albumin cluster is determined to be 600 mg metHb/kg (2.09 mg NaHS/kg).

3.3. Availability of H_2S-metHb-albumin cluster as the hydrogen sulphide donor in vivo

IRI occurs during the transient inhibition and subsequent resumption of blood supply to the occlusion site [27]. Hydrogen sulfide is a potential therapeutic agent for ameliorating the onset and progression of IRI, including liver and heart, in animal models [28]. Additionally, the microenvironment of focal sites in IRI exhibits a low pH due to metabolic acidosis, causing hypoxia[27], indicating that the H_2S-metHb-albumin cluster is superior to the conventional hydrogen sulphide donor, NaHS. Further, we confirmed the efficacy of the H_2S-metHb-albumin cluster as a hydrogen sulphide donor in hepatic IRI model mice and compared it to NaHS.

3.3.1 Therapeutic efficacy of H_2S-metHb-albumin cluster against hepatic IRI

To determine the clinical situation of liver transplantation and hepatic resection, hepatic IRI (70% ischemia) model mice were pre-injected with saline, H_2S-metHb-albumin clusters, or NaHS 30 min prior to the start of ischemia, and hepatic IRI was evaluated 6 h after reperfusion (Fig. 4a). Firstly, the optimal dose of H_2S-metHb-albumin cluster for hepatic IRI treatment was determined via *in vivo* experiments. Administrating the H_2S-metHb-albumin clusters

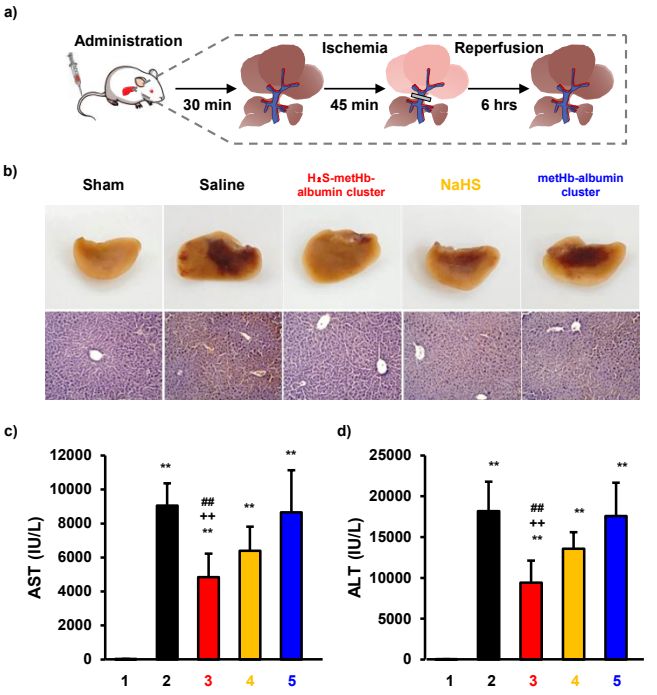

Figure 4 Protective effects of H_2S–metHb-albumin cluster in mice subjected to hepatic IRI. a) Schematic illustration of the experimental protocol for evaluating therapeutic efficacy against hepatic IRI, b) Representative gross photographs of the liver (top) and image of H&E-stained liver tissues (bottom) after IRI treatment. Plasma levels of c) AST and d) ALT. The numbers in the c) and d) indicate administered sample as follows: 1: sham, 2: saline, 3: H_2S–metHb-albumin cluster, 4: NaHS, and 5: metHb-albumin cluster. n = 6 per group, mean + S.D. **p < 0.01 vs. sham, ++p < 0.01 vs. saline, ##p < 0.01 vs. metHb-albumin cluster.

reduces plasma transaminase levels as their dose increases; however, the efficacy reaches the maximum at 300 mg metHb/kg (Fig. S1). Therefore, 300 mg metHb/kg of H_2S-metHb-albumin cluster and the equivalent sulphide dose of NaHS (1.05 mg NaHS/kg) were used for further *in vivo* experiments.

The therapeutic efficacy of the H_2S-metHb-albumin cluster against hepatic IRI was evaluated to assess its potential as a hydrogen sulphide donor compared to that of NaHS. As reported previously [29,30], liver damage after IRI, as determined by plasma transaminase levels and morphological observations, is ameliorated by the NaHS treatment (Fig. 4b–d). Further, the H_2S-metHb-albumin cluster restores the hepatic IRI, but the metHb-albumin cluster does not, indicating that hydrogen sulphide released from the H_2S-metHb-albumin cluster contributes to the therapeutic efficacy. The H_2S-metHb-albumin cluster treatment shows superior amelioration of hepatic IRI compared to NaHS treatment, even though equal quantities of hydrogen sulphide (1.05 mg/kg) are administered. Fig. 3 reveals that the H_2S-metHb-albumin cluster efficiently releases sulphides at low pH. Additionally, the metHb-albumin cluster, a scaffold for hydrogen sulphide, is well distributed in the liver with long blood retention [21]. The properties of the H_2S-metHb-albumin cluster enable a superior hydrogen sulphide delivery to the liver compared to that of NaHS. To corroborate this hypothesis, sulphide levels in focal sites of IRI after H_2S-metHb-albumin clustering and NaHS administration were compared. However, we could not quantify the exogenous sulphide levels in this study due to technical difficulties. This could be investigated in future studies to establish the effectiveness of the H_2S-metHb-albumin cluster as a hydrogen sulphide donor in response to low pH would be evaluated.

3.3.2 Protective mechanism of H_2S-metHb-albumin cluster against IRI

IRI initiates and progresses through various molecular mechanisms, including imbalanced oxidative and inflammatory responses [27]. Hydrogen sulphide comprehensively alleviates the oxidative and inflammatory conditions, ameliorating the hepatic IRI [31]. To corroborate the applicability of the H_2S-metHb-albumin cluster as a hydrogen sulphide donor, we determined hepatic responses after IRI, which are generally observed after hydrogen sulphide treatment.

Kang et al. reported that NaHS treatment suppressed MDA content, an oxidative injury marker, in the liver of the hepatic IRI model rats[30]. This report agrees with our results, wherein NaHS treatment suppresses MDA accumulation in the liver of IRI model mice (Fig. 5a). These suppressive effects are also observed in IRI model mice treated by the H_2S-metHb-albumin cluster. Further, hydrogen sulphide enhances antioxidant capacity owing to increased quantity of GSH, an *in vivo* antioxidant [32]. H_2S-metHb-albumin cluster treatment sustains significantly high hepatic GSH levels compared to that of the NaHS treatment (Fig. 5b). Moreover, H_2S-metHb-albumin cluster treatment significantly increases the GSH/GSSG ratio (Fig. 5c).

Overproduction of proinflammatory cytokines accelerates hepatic IRI[27]. As reported previously, exogenous supplementation with hydrogen sulphide suppressed inflammatory responses in hepatic IRI [33–35]. In this study, all the observed inflammatory cytokines levels, i.e., interleukin–1β (IL-1β), interleukin–6 (IL-6), tumour necrosis factor–α (TNF-α), and interferon-γ (IFN-γ) show a significant increase by the hepatic IRI induction (Fig. 6a–d). In contrast, plasma inflammatory cytokine levels significantly decrease in the H_2S-metHb-albumin cluster treatment group, which is more pronounced than that in the NaHS treatment group. TNF-α and IFN-γ levels in the H_2S-metHb-albumin cluster treatment group are approximately equal to those in the control (sham) group (Figs. 6c and d). It has been developed a better understanding of the mechanisms underlying the anti-inflammatory effects of hydrogen sulphide treatment. Other biological gaseous substances, carbon monoxide, suppress inflammatory cytokines *via* Kupffer cell inactivation [36]; therefore, H_2S-metHb-albumin cluster treatment can inactivate Kupffer cells and alleviate inflammatory reactions. In addition, the administration of metHb-albumin cluster, a scaffold of H_2S-metHb-albumin cluster, did not change the production of these inflammatory cytokines in healthy mice (Fig. S2), suggesting that H_2S-metHb-albumin cluster does not induce inflammation even after H_2S is released.

Hence, the H_2S-metHb-albumin cluster alleviates hepatic IRI via its antioxidative and anti-inflammatory effects, similar to the preventive mechanisms of NaHS. Additionally, it exhibits efficient hydrogen sulphide delivery to the liver, achieving superior therapeutic effects over those of NaHS.

3.4. Toxicity and biological compatibility of H_2S-metHb-albumin cluster

Administering 300 mg metHb/kg of H_2S-metHb-albumin cluster (equivalent to 1.05 mg NaHS/kg) is not lethal (Table 1); however, the

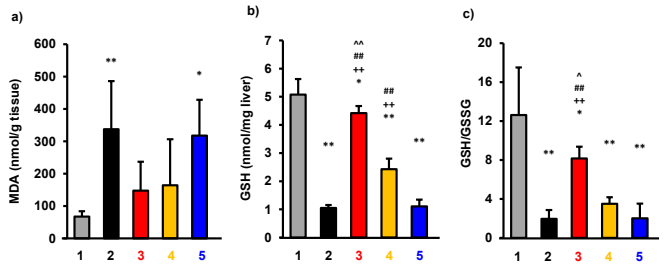

Figure 5 Hepatic oxidative responses after H_2S–metHb-albumin cluster administration in mice subjected to hepatic IRI. a) MDA levels, b) GSH, and c) GSH/GSSG ratio. n = 5–6 per group, mean + S.D. The numbers in the figures indicate the administered sample as follows: 1: sham, 2: saline, 3: H_2S–metHb-albumin cluster, 4: NaHS, and 5: metHb-albumin cluster. *p < 0.05, **p < 0.01 vs. sham, +p < 0.05, ++p < 0.01 vs. saline, ^p < 0.05, ^^p < 0.01 vs. NaHS, #p < 0.05, ##p < 0.01 vs. metHb-albumin cluster.

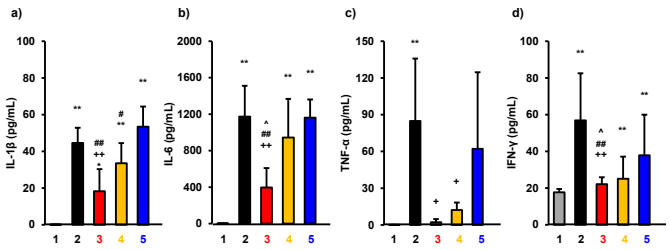

Figure 6 Inflammatory responses after administering H_2S–metHb-albumin cluster in the mice subjected to IRI. a) IL–1β, b) IL–6, c) TNF–α, and d) IFN–γ. n = 5–6 per group, mean + S.D. The numbers in the figures indicate the administered sample as follows: 1: sham, 2: saline, 3: H_2S–metHb-albumin cluster, 4: NaHS, and 5: metHb-albumin cluster. *p < 0.05, **p < 0.01 vs. sham, +p < 0.05, ++p < 0.01 vs. saline, ^p < 0.05, ^^p < 0.01 vs. NaHS, #p < 0.05, ##p < 0.01 vs. metHb-albumin cluster.

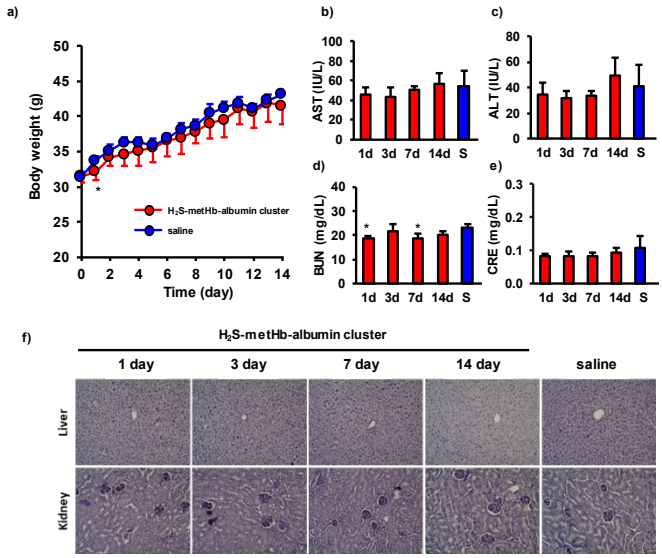

Figure 7 Biological responses after H_2S–metHb-albumin cluster administration in healthy mice. a) Body weight (n = 4–20, mean ± S.D.) Plasma levels of b) AST, c) ALT, d) BUN, and e) CRE. (n = 4, mean + S.D.) f) Representative morphological images stained by H&E. (×200 magnification) H_2S–metHb-albumin cluster (300 mg metHb/kg) was administered to healthy mice (n = 20). Four mice were sacrificed to harvest biological samples for evaluation on days 1, 3, 7, and 14. Mice receiving saline were sacrificed on day 14 (n = 4). *p < 0.05 vs. saline. S: saline

non-lethal toxic effect of hydrogen sulphide released from H_2S-metHb-albumin cluster, on normal tissues is concerning. The alternative energy production upon hydrogen sulphide intoxication is attributed to impaired oxygen utilization by cytochrome *c* oxidase. Therefore, the clinical symptoms of hydrogen sulphide intoxication include hypoxia and metabolic acidosis[37]. Hence, we determined the acidosis-related blood gas and cytochrome *c* oxidase activity in organs after administering 300 mg metHb/kg H_2S-metHb-albumin cluster (equivalent to 1.05 mg NaHS/kg) to healthy mice. The acidosis-related blood gas parameters (pH, bicarbonate, lactate, and base excess) remain unchanged (Fig. S3). Additionally, no reduction in cytochrome *c* oxidase activity is observed in any of the organs (Fig. S4), indicating that the H_2S-metHb-albumin cluster does not induce non-lethal intoxication symptoms caused by hydrogen sulphide.

Further, biological responses were monitored for up to 14 days after the administration of H_2S-metHb-albumin cluster (300 mg metHb/kg) to confirm the biological compatibility. The body weight of H_2S-metHb-albumin cluster-treated mice increases over time, comparable to that of saline-treated mice (Fig. 7a). The biochemistry reflecting hepatic (AST, ALT, total protein, albumin, and albumin/globulin ratio) and renal functions (blood urea nitrogen (BUN) and creatinine (CRE)) does not exhibit any significant changes. Further, no abnormal morphological changes are observed (Figs. 7b–f, Fig. S5). In previous reports, we observed no abnormal changes in clinical chemistries and morphology reflecting renal injury, heart injury, or hepatic injury, haematocytes, electrolytes, blood gas parameters after administering higher doses of the metHb-albumin cluster (up to 600 mg metHb/kg)[21]. Additionally, the metHb-albumin cluster metabolizes *via* the endogenous metabolic pathways of albumin and Hb because they are the biological components [21], and hydrogen sulphide metabolizes in a similar manner to that of endogenous hydrogen sulphide, which involves methylation and oxidation to thiosulfate [38]. These suggest that the H_2S-metHb-albumin cluster does not induce abnormal responses such as organ injuries and haemotoxicity even after the release of H_2S. Hence, the H_2S-metHb-albumin cluster is a biocompatible hydrogen sulphide donor with good metabolic properties.

Conclusions

This study successfully demonstrates the proof-of-concept that the H_2S-metHb-albumin cluster is a potent and superior hydrogen sulphide donor over NaHS, the conventional hydrogen sulphide donor. Stimuli-triggered hydrogen donors have been developed using synthetic chemicals and materials such as polymers owing to the non-specific hydrogen sulphide delivery and safety concerns of NaHS [39–43]. However, most of these hydrogen sulphide donors consist of abiotic substances, which can result in unexpected biological responses and environmental pollution. In contrast, the H_2S-metHb-albumin cluster developed in this study is of biological origins, comprising Hb and albumin. Furthermore, owing to the inherent relationship between hydrogen sulphide and metHb, the H_2S-metHb-albumin cluster provides a sustained release of hydrogen sulphide at a low pH. This pH-responsive property of the H_2S-metHb-albumin cluster facilitates its availability and applicability as a hydrogen sulphide donor for medication, especially for disorders where the microenvironment is in a state of low pH. These findings open new avenues for utilizing metHb-based materials, including metHb-albumin clusters, for medical applications using hydrogen sulphide delivery.

Author contributions

Yuto Suzuki: Investigation, Formal Analysis, Funding acquisition, and Writing- Original draft preparation. Taiga Yamada: Resources, Formal Analysis, and Investigation. Yuki Enoki: Investigation and Formal Analysis. Kazuaki Matsumoto: Project administration, and Writing – review & editing, Teruyuki Komatsu: Conceptualization, Project administration, Writing – review & editing, and Supervision. Kazuaki Taguchi: Conceptualization, Project administration, Investigation, Formal Analysis, Funding acquisition, Writing – review & editing, and Supervision.

Conflicts of interest

There are no conflicts to declare.

Data availability

All data generated or analysed during this study are included in this published article and its supporting information.

Acknowledgements

This work was supported by JST SPRING (grant number JPMJSP2123) and The Keio University Doctorate Student Grant-in-Aid Program from the Ushioda Memorial Fund.

References

1 K. Abe and H. Kimura, *J Neurosci*, 1996, **16**, 1066–1071.

2 W. Guo, Z. Y. Cheng and Y. Z. Zhu, *Acta Pharmacol Sin*, 2013, **34**, 1284–1291.

3 J. A. Machado-Neto, A. R. Azevedo Cerqueira, S. Veríssimo-Filho, M. N. Muscará, S. K. Pereira Costa and L. R. Lopes, *Antioxid Redox Signal*, 2024, **40**, 250–271.

4 H. J. Sun, Z. Y. Wu, X. W. Nie, X. Y. Wang and J. S. Bian, *J Adv Res*, 2020, **27**, 127–135.

5 A. H. Sharif, M. Iqbal, B. Manhoosh, N. Gholampoor, D. Ma, M. Marwah and L. Sanchez-Aranguren, *Neurochem Res*, 2023, **48**, 1981–1996.

6 Y. Song, S. Wu, R. Zhang, Q. Zhong, X. Zhang and X. Sun, *Front Pharmacol*, 2024, **15**, 1336693.

7 S. Ali Akbari Ghavimi, T. J. Faulkner, R. R. Tata, A. J. Hemmerla, S. E. Huddleston, F. Rezaei, E. S. Lungren, R. Zhang, E. E. Bumann and B. D. Ulery, *Pharmaceuticals (Basel)*, 2024, **17**, 585.

8 Z. He, Y. Zhu, H. Ma, Q. Shen, X. Chen, X. Wang, H. Shao, Y. Wang and S. Yang, *Int Immunopharmacol*, 2024, **132**, 111990.

9 S. Zhang, M. Wang, H. Li, Q. Li, N. Liu, S. Dong, Y. Zhao, K. Pang, J. Huang, C. Ren, Y. Wang, Z. Tian, F. Lu and W. Zhang, *J Cachexia Sarcopenia Muscle*, 2023, **14**, 2719–2732.

10 S. Zhang, J. Shen, Y. Zhu, Y. Zheng, W. San, D. Cao, Y. Chen and G. Meng, *Biochem Pharmacol*, 2023, **215**, 115748.

11 X. Zhang, K. Cui, X. Wang, Y. Tong, C. Liu, Y. Zhu, Q. You, Z. Jiang and X. Guo, *Antioxidants (Basel)*, 2023, **12**, 1062.

12 Z. W. Lee, X. Y. Teo, E. Y. W. Tay, C. H. Tan, T. Hagen, P. K. Moore and L. W. Deng, *Br J Pharmacol*, 2014, **171**, 4322–4336.

13 Z. W. Lee, J. Zhou, C. S. Chen, Y. Zhao, C. H. Tan, L. Li, P. K. Moore and L. W. Deng, *PLoS One*, 2011, **6**, e21077.

14 C. T. Yang, L. Chen, S. Xu, J. J. Day, X. Li and M. Xian, *Front Pharmacol*, 2017, **8**, 664.

15 J. Fan, E. Pung, Y. Lin and Q. Wang, *Biomaterials translational*, 2022, **3**, 250–263.

16 B. Jensen and A. Fago, *J Inorg Biochem*, 2018, **182**, 133–140.

17 Y. Suzuki, Y. Arakida, H. Sakai, Y. Enoki, K. Matsumoto and K. Taguchi, *Toxicol Appl Pharmacol*, 2023, **481**, 116752.

18 K. Taguchi, T. Maruyama and M. Otagiri, *Drug Metab Rev*, 2011, **43**, 362–373.

19 Y. Suzuki, K. Taguchi, T. Kure, H. Sakai, Y. Enoki, M. Otagiri and K. Matsumoto, *J Control Release*, 2021, **337**, 59–70.

20 M. Kristiansen, J. H. Graversen, C. Jacobsen, O. Sonne, H. J. Hoffman, S. K. A. Law and S. K. Moestrup, *Nature*, 2001, **409**, 198–201.

21 Y. Suzuki, K. Taguchi, W. Okamoto, Y. Enoki, T. Komatsu and K. Matsumoto, *J Control Release*, 2022, **349**, 304–314.

22 R. Funaki, T. Kashima, W. Okamoto, S. Sakata, Y. Morita, M. Sakata and T. Komatsu, *ACS Omega*, 2019, **4**, 3228–3233.

23 Y. Abe, I. Hines, G. Zibari, K. Pavlick, L. Gray, Y. Kitagawa and M. Grisham, *Free Radic Biol Med*, 2009, **46**, 1–7.

24 Y. Suzuki, K. Taguchi, W. Okamoto, Y. Enoki, T. Komatsu and K. Matsumoto, *Int J Pharm*, 2023, **645**, 123433.

25 Y. Suzuki, K. Taguchi, S. Hanyu, T. Kure, Y. Enoki, M. Otagiri, H. Sakai and K. Matsumoto, *J Drug Deliv Sci Technol*, 2022, **71**, 103282.

26 S. W. Borron and V. S. Bebarta, *Emerg Med Clin North Am*, 2015, **33**, 89–115.

27 M.-Y. Wu, G.-T. Yiang, W.-T. Liao, A. P.-Y. Tsai, Y.-L. Cheng, P.-W. Cheng, C.-Y. Li and C.-J. Li, *Cellular physiology and biochemistry : international journal of experimental cellular physiology*, 2018, **46**, 1650–1667.

28 A. L. King and D. J. Lefer, *Exp Physiol*, 2011, **96**, 840–846.

29 E. M. Bos, P. M. Snijder, H. Jekel, M. Weij, J. C. Leemans, M. C. F. van Dijk, J.-L. Hillebrands, T. Lisman, H. van Goor and H. G. D. Leuvenink, *Transplant International*, 2012, **25**, 897–908.

30 K. Kang, M. Zhao, H. Jiang, G. Tan, S. Pan and X. Sun, *Liver Transplantation*, 2009, **15**, 1306–1314.

31 B. Liu, S. Wang, M. Xu, Y. Ma, R. Sun, H. Ding and L. Li, *Front Pharmacol*, 2022, **13**, 899859.

32 S. Jha, J. W. Calvert, M. R. Duranski, A. Ramachandran and D. J. Lefer, *American Journal of Physiology-Heart and Circulatory Physiology*, 2008, **295**, H801–H806.

33 M. Lu, X. Jiang, L. Tong, F. Zhang, L. Ma, X. Dong and X. Sun, *Biol Pharm Bull*, 2018, **41**, 229–238.

34 D. Wang, Y. Ma, Z. Li, K. Kang, X. Sun, S. Pan, J. Wang, H. Pan, L. Liu, D. Liang and H. Jiang, *Autophagy*, 2012, **8**, 954–962.

35 S. A. Ibrahim, S. A. Abdel-Gaber, M. A. Ibrahim, E. F. Amin, R. K. Mohammed and A. M. Abdelrahman, *Curr Mol Pharmacol*, 2022, **15**, 676–682.

36 S. Ogaki, K. Taguchi, H. Maeda, H. Watanabe, Y. Ishima, M. Otagiri and T. Maruyama, *Biochem Pharmacol*, 2015, **97**, 310–319.

37 P. C. Ng, T. B. Hendry-Hofer, A. E. Witeof, M. Brenner, S. B. Mahon, G. R. Boss, P. Haouzi and V. S. Bebarta, *J Med Toxicol*, 2019, **15**, 287–294.

38 A. L. King and D. J. Lefer, *Exp Physiol*, 2011, **96**, 840–846.

39 K. Kaur, R. J. Carrazzone and J. B. Matson, *Antioxid Redox Signal*, 2020, **32**, 79–95.

40 A. Sikder, R. Mengji, S. Mondal, A. Jana and N. D. P. Singh, *J Mater Chem B*, 2023, **11**, 5131–5141.

41 Z. Wang, Y. Tang, M. Gao, X. Bai, Y. Li, X. Hao, Y. Lu and X. Zhou, *ACS Macro Lett*, 2023, **12**, 1583–1588.

42 X. Dong, H. Zhang, P. Duan, K. Liu, Y. Yu, W. Wei, W. Wang, Y. Liu, Q. Cheng, X. Liang, Y. Huo, L. Yan, A. Yu and H. Dai, *Sci Adv*, 2023, **9**, eadi1078.

43 F. Yuan, X. He, Y. Lu, L. Ning, X. Zhao, S. Zhang, F. Guan, Y. Guo and J. Zhang, *Anal Chem*, 2023, **95**, 6931–6939.

Data availability statement

All data generated or analysed during this study are included in this published article and its supporting information.